



Article

Cerebral Folate Metabolism in Post-Mortem Alzheimer's Disease Tissues: A Small Cohort Study

Naila Naz ¹, Syeda F. Naqvi ¹ , Nadine Hohn ¹, Kiara Whelan ¹ , Phoebe Littler ¹, Federico Roncaroli ^{1,2} , Andrew C. Robinson ^{1,2} and Jaleel A. Miyan ^{1,*}

¹ Division of Neuroscience, School of Biological Sciences, Faculty of Biology, Medicine & Health, The University of Manchester, 3.540 Stopford Building, Oxford Road, Manchester M13 9PT, UK

² Geoffrey Jefferson Brain Research Centre, Manchester Academic Health Science Centre (MAHSC), The University of Manchester, Salford Royal Hospital, Salford M6 8HD, UK

* Correspondence: j.miyam@manchester.ac.uk; Tel.: +44-161-306-4205

Abstract: We investigated the cerebral folate system in post-mortem brains and matched cerebrospinal fluid (CSF) samples from subjects with definite Alzheimer's disease (AD) ($n = 21$) and neuropathologically normal brains ($n = 21$) using immunohistochemistry, Western blot and dot blot. In AD the CSF showed a significant decrease in 10-formyl tetrahydrofolate dehydrogenase (FDH), a critical folate binding protein and enzyme in the CSF, as well as in the main folate transporter, folate receptor alpha (FR α) and folate. In tissue, we found a switch in the pathway of folate supply to the cerebral cortex in AD compared to neurologically normal brains. FR α switched from entry through FDH-positive astrocytes in normal, to entry through glial fibrillary acidic protein (GFAP)-positive astrocytes in the AD cortex. Moreover, this switch correlated with an apparent change in metabolic direction to hypermethylation of neurons in AD. Our data suggest that the reduction in FDH in CSF prohibits FR α -folate entry via FDH-positive astrocytes and promotes entry through the GFAP pathway directly to neurons for hypermethylation. This data may explain some of the cognitive decline not attributable to the loss of neurons alone and presents a target for potential treatment.

Keywords: Alzheimer's disease; cerebral folate; folate metabolism; cerebrospinal fluid; ALDH1L1; astrocytes; neurons; methylation



Citation: Naz, N.; Naqvi, S.F.; Hohn, N.; Whelan, K.; Littler, P.; Roncaroli, F.; Robinson, A.C.; Miyan, J.A. Cerebral Folate Metabolism in Post-Mortem Alzheimer's Disease Tissues: A Small Cohort Study. *Int. J. Mol. Sci.* **2023**, *24*, 660. <https://doi.org/10.3390/ijms24010660>

Academic Editors: Anna Atlante and Balazs Pal

Received: 23 November 2022

Accepted: 27 December 2022

Published: 30 December 2022



Copyright: © 2022 by the authors. Licensee MDPI, Basel, Switzerland. This article is an open access article distributed under the terms and conditions of the Creative Commons Attribution (CC BY) license (<https://creativecommons.org/licenses/by/4.0/>).

1. Introduction

Alzheimer's disease (AD) is an irreversible neurodegenerative condition affecting around 40 million people over the age of 60, with numbers reportedly doubling every 20 years, worldwide [1]. More than 2000 clinical trials, aimed to slow or halt the disease have failed [2–5]. These trials were based on different hypotheses of disease aetiology, pathogenesis and progression and likely failed because intervention happened too late in the course of the disease. Given the personal, social and economic burden of AD, there is an urgent need to identify novel approaches to the condition. Cerebral folate metabolism is one potential new and promising target.

Folate is absorbed across the gut and transported to the whole body by folate receptor alpha (FOLR1 or FR α) which is the main transporter and carries folate across the choroid plexus into the cerebrospinal fluid (CSF) [6]. Aldehyde dehydrogenase-1L1 (ALDH1L1), also known as 10-formyl tetrahydrofolate dehydrogenase (FDH), is a key folate binding protein and enzyme involved in many functions including tumour suppression [7–10]. Specific forms of epilepsy, a form of autism and a related severe neurological condition, named cerebral folate deficiency syndrome (CFD) are caused by maternal autoantibodies to FR α that block the transfer of folate from foetal blood into the foetal brain leading to profound folate deficiency and resulting in poor development and progressively severe neurological signs and symptoms after birth [11–18]. Furthermore, CSF drainage impairment has been directly linked to cerebral folate deficiency or imbalance with the extreme

case of hydrocephalus showing a blockade of available folate in the CSF by the withdrawal of the folate-binding protein, FDH from CSF [19].

Metabolic deficiencies have been highlighted as one of the potential causes of AD [2]. Our recent study demonstrated that single nucleotide polymorphisms (SNPs) affecting the folate enzyme methylene tetrahydrofolate dehydrogenase 1 (MTHFDH1) were significantly associated with AD and were also found to have resulted in a shift in folate metabolism [20]. Folate deficiency either due to CFD or folate imbalance resulting from CSF drainage insufficiency is associated with a multitude of conditions including AD. Silverberg and colleagues demonstrated both reduced CSF production as well as enlargement of the ventricles in Alzheimer's patients [21–23]. In addition, they found that CSF turnover rate decreases in normal ageing associated with amyloid deposition [24]. In other neurological conditions, including benign external hydrocephalus associated with autism, the large head size is associated with CSF accumulation both outside the brain, in the subarachnoid space [25–27], and also inside the brain associated with enlarged ventricles [25,28]. Significantly, disease severity has also been associated with increased ventricular enlargement in AD [29–32] indicating a potential common mechanism in conditions affecting the cerebral cortex and suggesting a common CSF turnover and cerebral folate metabolic link to many cerebral conditions. This is reinforced by a recent report detailing changes in methylation as well as changes in polyamine pathways in AD, that are intimately linked to folate metabolism [33], as well as the critical review of Liu et al. (2019) [2] and our own studies identifying an abnormality in a gene for a folate enzyme [20]. The current study, therefore, investigated the cerebral folate system in post-mortem brains and matched CSF of those considered neuropathologically normal for age (Braak stage 0-II) and those with neuropathologically confirmed AD (Braak stage V-VI). We, and others, have previously shown that FR α and FDH are involved in the transport and exchange of folate across the blood-CSF barrier and delivery to the brain across the CSF-brain barrier [34–37]. We have also shown that reduced FDH in CSF is associated with a cell cycle arrest in neural stem/progenitor cells in hydrocephalus [38,39]. We therefore initially focused on these molecules and aimed to identify any changes in the supply, transport and metabolism of folate in the AD group as compared to neuropathologically normal control group.

2. Results

2.1. Cerebrospinal Fluid (CSF) Analysis

Western blot analysis of CSF from the AD group (Braak V-VI) demonstrated a significant decrease in FDH protein expression as compared to the neurologically normal group (Braak 0-II; Figure 1).

FDH was significantly reduced in AD compared to normal with a statistical significance of $p \leq 0.0001$. Similarly, FR α ($p = 0.0308$) and folate ($p = 0.0011$) were also significantly reduced in AD (Figure 1). The raw optical density values for each parameter studied are given in tabular form in Figure 1. This reduction in folate related proteins and metabolites indicates a decreased folate supply, by FR α transport from the blood across the choroid plexus, as well as a general downregulation in folate metabolism in CSF of AD patients. Full gels and membranes are illustrated in Supplementary Figure S1.

2.2. Immunohistochemistry for Cerebral Cortex

In normal brain, FDH-positive cells form a network from the top of the cortex, where they connect to the pia mater (Figure 2a) right through to the ependymal lining of the ventricles. These FDH⁺ cells have different morphologies in different cortical regions; classical stellate morphology in the cortex (Figure 2b,c), small and thin with short processes in the white matter (Figure 2d), large and more rounded with short processes in the sub-ventricular zone (Figure 2e) and with longer processes in the ventricular zone (Figure 2f) looking more like the classical stellate morphology.

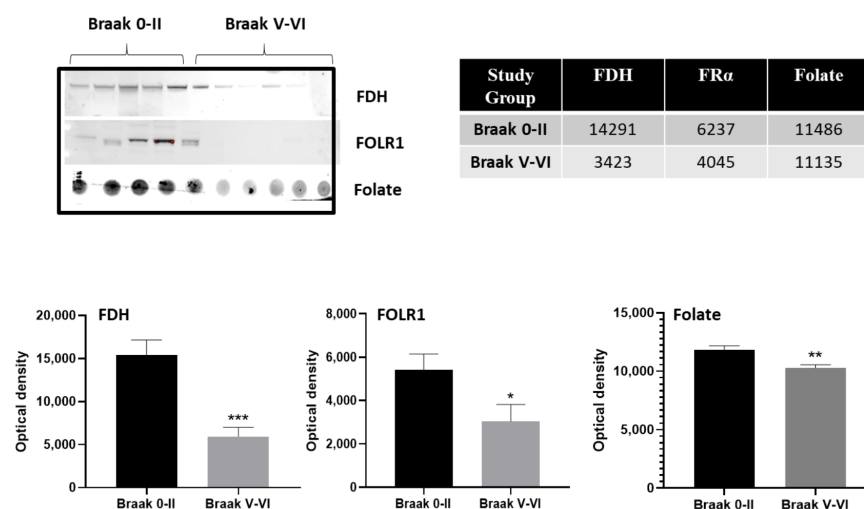


Figure 1. Western and dot blot analysis of CSF for FDH, FR α and folate. The images of the relevant bands and dots from different blots for FDH, FR α and folate are shown at top with optical density measurements plotted as mean \pm SEM for $n = 21$ per group. *, ** and *** show significance at $p < 0.05$, 0.001, and 0.0001, respectively. The mean optical density measurements are shown in the table. Images of the full blot membranes are shown in Supplementary Figure S1.

Since FDH is a recognised marker of astrocytes, the nature of these FDH⁺ cells was further confirmed by co-localisation with the astrocyte markers S100 and GFAP (Figure 3). Both markers have variable intensities of co-localisation. Moreover, they share selective sub-cellular co-localisation with FDH⁺ astrocytes indicating changes between markers potentially depending on localised functional requirements. To elaborate, adjacent areas of cortex, associated with the pia mater, were observed to be FDH⁺/GFAP⁻ (Figure 3a) or FDH⁻/GFAP⁺ (Figure 3b). In other parts of the cortex, GFAP⁺/FDH⁺ astrocytes were observed with their GFAP⁺/FDH⁺ end feet over the surface of a capillary (Figure 3c). Next to it, FDH⁺/GFAP⁻ were observed with FDH⁺/GFAP⁻ end feet on the surface of a neighbouring capillary (Figure 3c). Additionally, areas of cortex (Figure 3b) and ependymal (Figure 3e) demonstrated very few GFAP⁺/FDH⁺ astrocytes. Similar to these observations in the cortical marginal zone, we found regions of the ventricular zone and ependyma that had adjacent areas of FDH⁺/GFAP⁻ or FDH⁻/GFAP⁺ glial processes (Figure 3f). In the cortex, the FDH⁺ cells also demonstrated colocalisation with S100 (Figure 3g). FR α and GFAP demonstrated limited colocalisation most notably in the marginal zone of the cortex (Figure 3h). Micrographs taken with each separate wavelength for this, and subsequent figures, are shown in Supplementary Figures S2–S6.

Double immunostaining for FDH and FR α in normal and AD brains showed a striking and substantial change in distribution of these two folate related proteins (Figure 4). In normal brains, cortical cells were found to be FDH⁺/FR α ⁺ with a stronger colocalisation in cells extending to the pia mater (Figure 4a). Additionally, FR α staining appeared as speckles within what we believe to be neuronal cells (white arrows in Figure 4b) reflecting its transport through endocytic vesicles where the FDH⁺/FR α ⁺ astrocytes also appeared to have close associations with these (Figure 4b). In contrast, in AD brain, most cells were either FDH⁺/FR α ⁻ or FDH⁻/FR α ⁺ indicating that the cortical expression of FR α and FDH has become almost completely separated. Very few cells maintain FDH⁺/FR α ⁺ indicating that only a few FDH⁺ astrocytes still have positive staining for FR α (Figure 4c–e) and thus retain transport capability for FR α and folate. The FDH⁺ astrocytes in AD brain have more extensive and denser processes than in normal brain (Figure 4b,d). To identify the other cell type positive for FR α , double immunofluorescence staining with the neuronal nucleus marker (NeuN) was performed. In normal brain cortex, a few cells were found to be FR α ⁺/NeuN⁺, indicating FR α related folate supply is probably low to neuronal cells (Figure 4f–h). However, in AD brain, many cortical cells were seen to be FR α ⁺/NeuN⁺

(Figure 4i,k) indicating that $FR\alpha$ is concentrated into neuronal cell bodies throughout the cortex in AD.

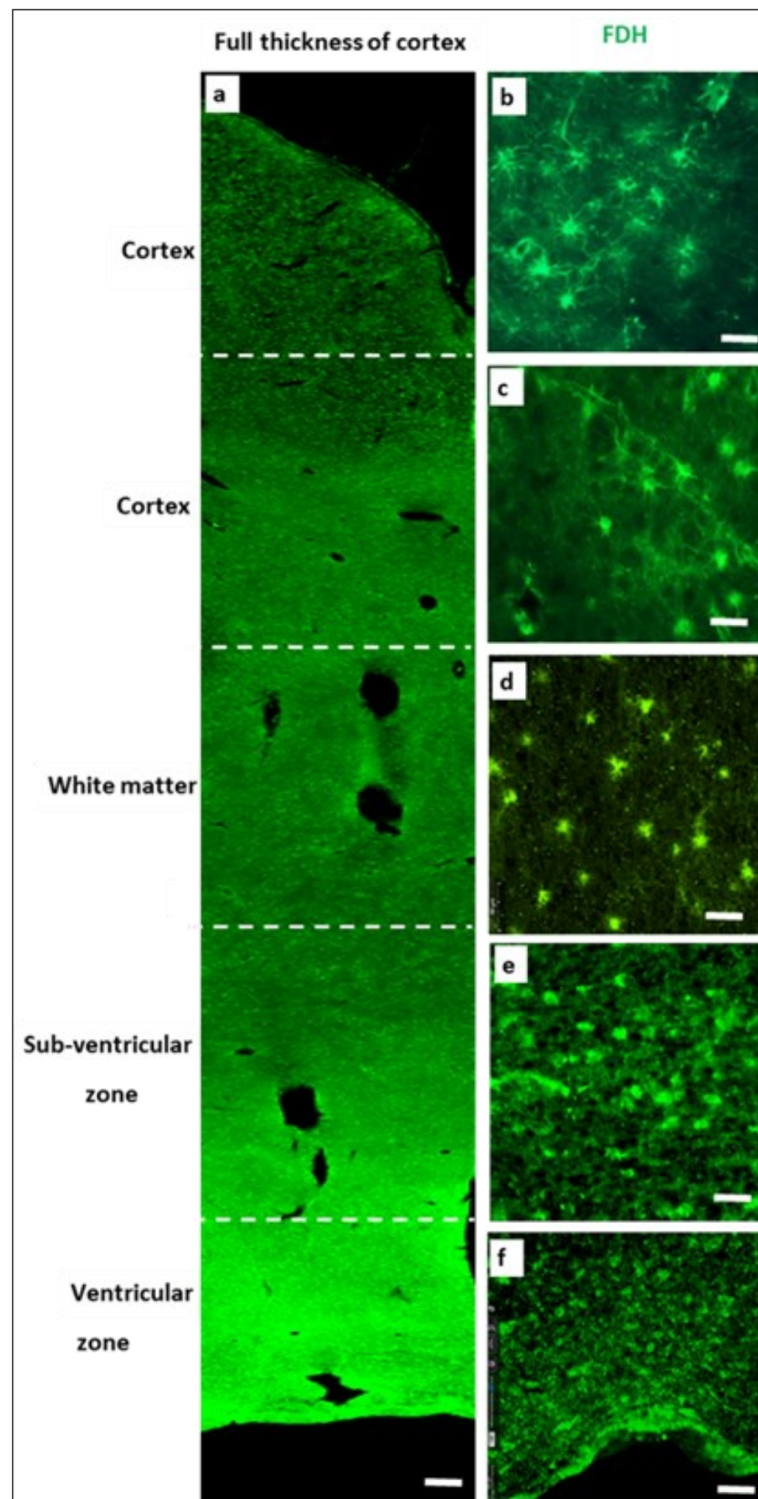


Figure 2. Immunofluorescence staining of Braak 0-II brain sections for FDH (green). Left panel (a) shows the entire section of cortex shown at low power ($5\times$; scale bar: 2 mm) to orientate the different regions of brain shown in the right panels (b–f) at $200\times$, scale bar: $50\ \mu\text{m}$. (b) Cortex near the pia mater, (c) Mid cortex region, (d) White matter region, (e) sub-ventricle zone, (f) ventricular zone. The image is representative of $n = 3$ brains.

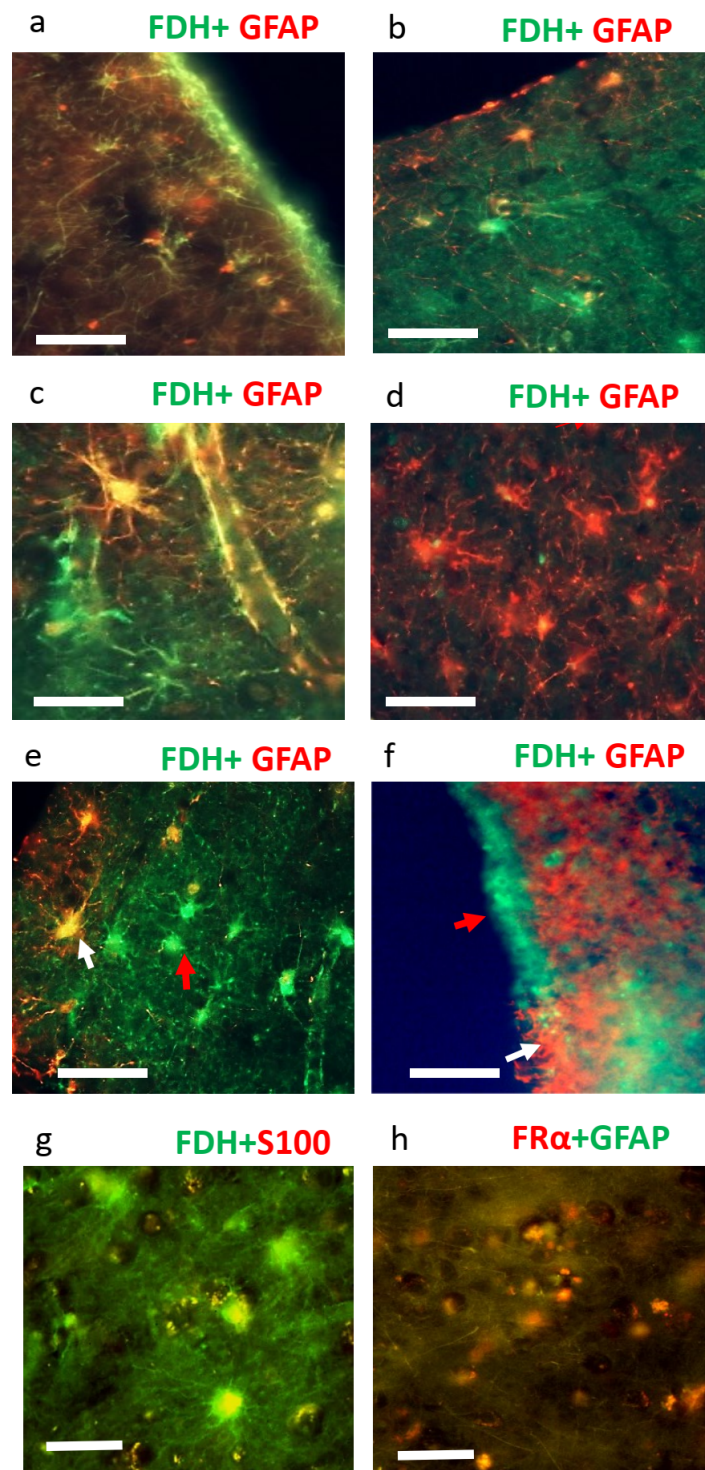


Figure 3. Immunofluorescence staining of Braak 0-II brain for FDH, GFAP, FR α and GFAP. Double immunofluorescence for FDH (green) and GFAP (red) staining of neurologically normal brain in cortical region near the pia mater (**a,b**) 100 \times , scale: 100 μ m, white matter region (**c**), sub ventricular zone (**d**) and ventricular zone (**e,f**) at 200 \times , scale: 50 μ m. The white arrows indicate FDH⁺/GFAP⁺ whereas red arrow indicates FDH⁻/GFAP⁻. Double immunofluorescence staining of FDH (green) and S100 (red) (**g**) to demonstrate FDH⁺/S100⁺ astrocytes 200 \times , scale: 50 μ m. Double immunofluorescence staining for FR α and GFAP (**h**, 100 \times ; scale bar 100 μ m). The figure is representative of $n = 3$.

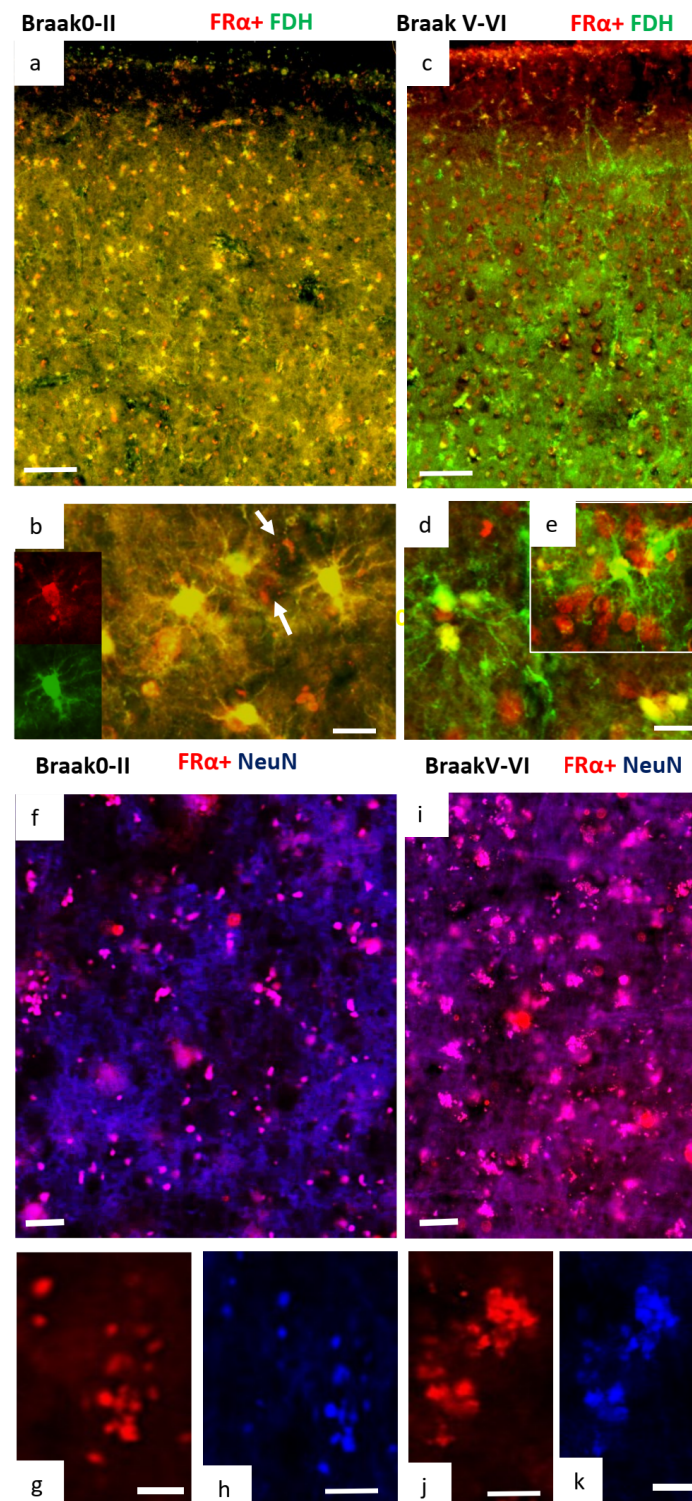


Figure 4. Immunofluorescence staining for FDH, FR α and NeuN. Double immunofluorescence staining for FR α (red) and FDH (green) in Braak 0-II (a,b) and Braak V-VI (c–e) brains ((a,c) 100 \times , scale:100 μ m and (b) 400 \times , 20 μ m). Co-localisation (yellow) of FR α with FDH in the FDH-positive astrocytes in normal brains (a,b) shows almost complete separation in Alzheimer brain (c–e). FR α appears as speckled red staining in normal neuronal cell bodies (white arrows in (b)) while in Alzheimer cortex these cells are full of red, FR α (d,e). Double immunofluorescence staining for FR α (red) and NeuN (blue) in normal (f) and AD (i) brains show colocalisation, which is shown in separate channels in (g,h) and (j,k) ((f), 200 \times , scale: 50 μ m ((g,h,j,k), 400 \times , scale: 20 μ m). The figure is representative of neurologically normal, Braak 0-II $n = 3$ and AD, Braak V-VI $n = 4$.

In normal brain, a strong expression of GFAP⁺/FDH⁺ in cells was observed with a few cells FR α ⁺/GFAP⁺ indicating that most GFAP positive astrocytes were strongly positive for FDH and least positive for FR α . In contrast, in AD brain, although some cells were FDH⁺/GFAP⁺ but mostly cells were found to be FR α ⁺/GFAP⁺ indicating a clear switch in signal from FDH positive astrocytes to FR α positive astrocytes. This switch was more obvious near to the pia mater in cortex (Figure 5).

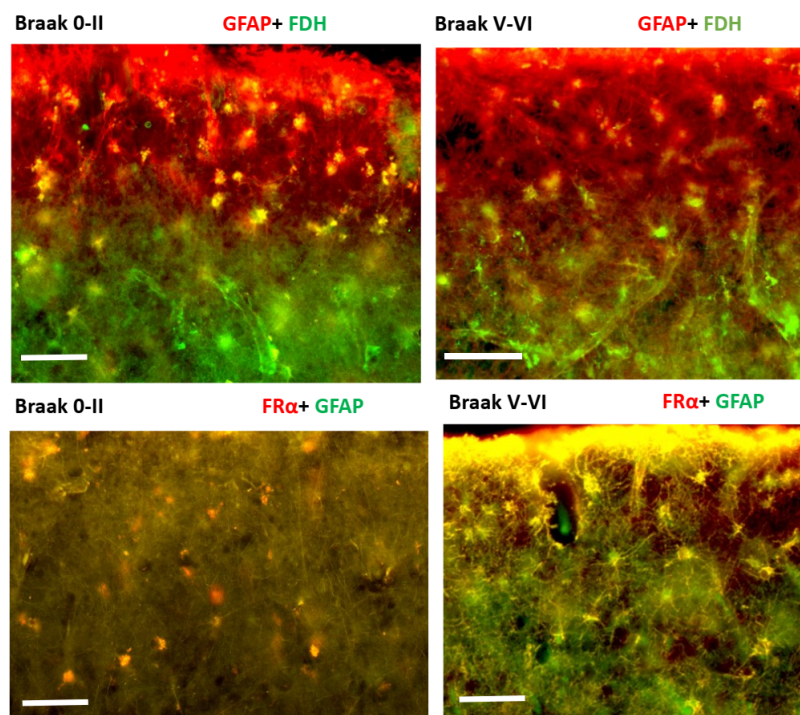


Figure 5. Immunofluorescence staining for GFAP, FR α and FDH. Upper panel: Double immunofluorescence staining for FDH (green) and GFAP (red) in normal and AD brains. Co-localisation (yellow) is observed in astrocytes. Lower panel: Double immunofluorescence staining for FR α (red) and GFAP (green) in neurologically normal and AD brains. Co-localisation is observed as bright yellow colour. Magnification 200 \times , scale bar: 50 μ m. The figure is representative of neurologically normal $n = 3$ and AD brains $n = 4$.

In the normal brain, most of the cortical cells are FDH⁺/folate⁺ (Figure 6a,b) and FR α ⁺/folate⁻ (Figure 6f,g) indicating folate transport by FR α through the FDH⁺ network of astrocytes. By contrast, in AD brain, cortical cells appeared to have two set of populations FDH⁻/Folate⁺ and a few FDH⁺/Folate⁺ (Figure 6c,d). A large number of cells were found to be FR α ⁺/folate⁺ (Figure 6h,i) which seems to be correlated with the FDH⁻/Folate⁺ cells (Figure 6c–e). Overall, this data set indicated a switch in folate transport pathway from FDH⁺/FR α ⁺/folate⁺/GFAP⁻ astrocytes in normal brain to FR α ⁺/folate⁺/GFAP⁺ astrocytes that are associated with NeuN⁺ neurons in AD brain.

2.3. Changes in Methylation in Neuronal Cells of Alzheimer's Disease Brain

In the normal brain, with some regional differences, most of the cortical cell population was positive for both 5mC and 5hmC. (Figure 7a,b). In contrast, AD brain cortical cells demonstrated very little colocalisation of 5mC and 5hmC. Essentially, most cells were found to be 5mC⁺/5hmC⁻ (Figure 7c,d). This was particularly evident in cells near the pia mater. This pattern of 5mC⁺/5hmC⁻ was in line with FDH⁻/FR α ⁺/folate⁺/NeuN⁺ cells near the pia mater as shown in Figure 4. The 5mC⁺ cells demonstrated colocalisation with the neuronal marker NeuN in normal and AD (Figure 7e–j). The data indicate that in AD brain, the cortical cells, particularly neurons, are hypermethylated, presumably due to FR α related transport of folate into the nuclei of neuronal cells.

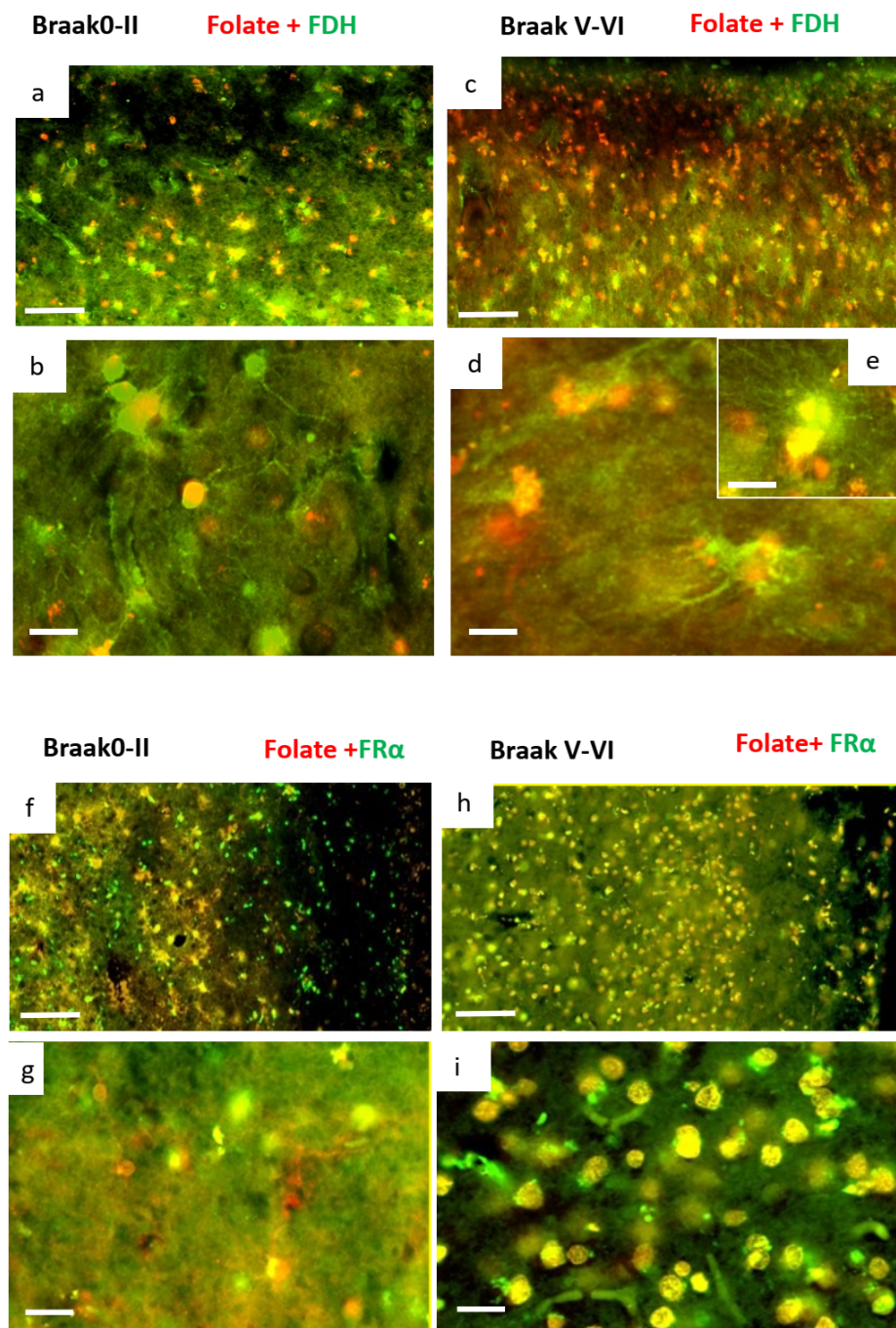


Figure 6. Immunofluorescence staining for folate, FR α and FDH. Double immunofluorescence staining for FDH (green) and folate (red) in neurologically normal ((a) $100 \times 100 \mu\text{m}$ and (b) $400 \times 20 \mu\text{m}$) and AD brain ((c) $100 \times 100 \mu\text{m}$ and (d) $400 \times 20 \mu\text{m}$). Some co-localisation (yellow) of folate and FDH ((e) $400 \times 20 \mu\text{m}$) is observed. Double immunofluorescence staining for FR α (green) and folate (red) in normal ((f) $100 \times 100 \mu\text{m}$ and (g) $400 \times 20 \mu\text{m}$) and AD brain ((h) $100 \times 100 \mu\text{m}$ and (i) $400 \times 20 \mu\text{m}$). The figure is representative of neurologically normal $n = 3$ and AD $n = 4$ brains.

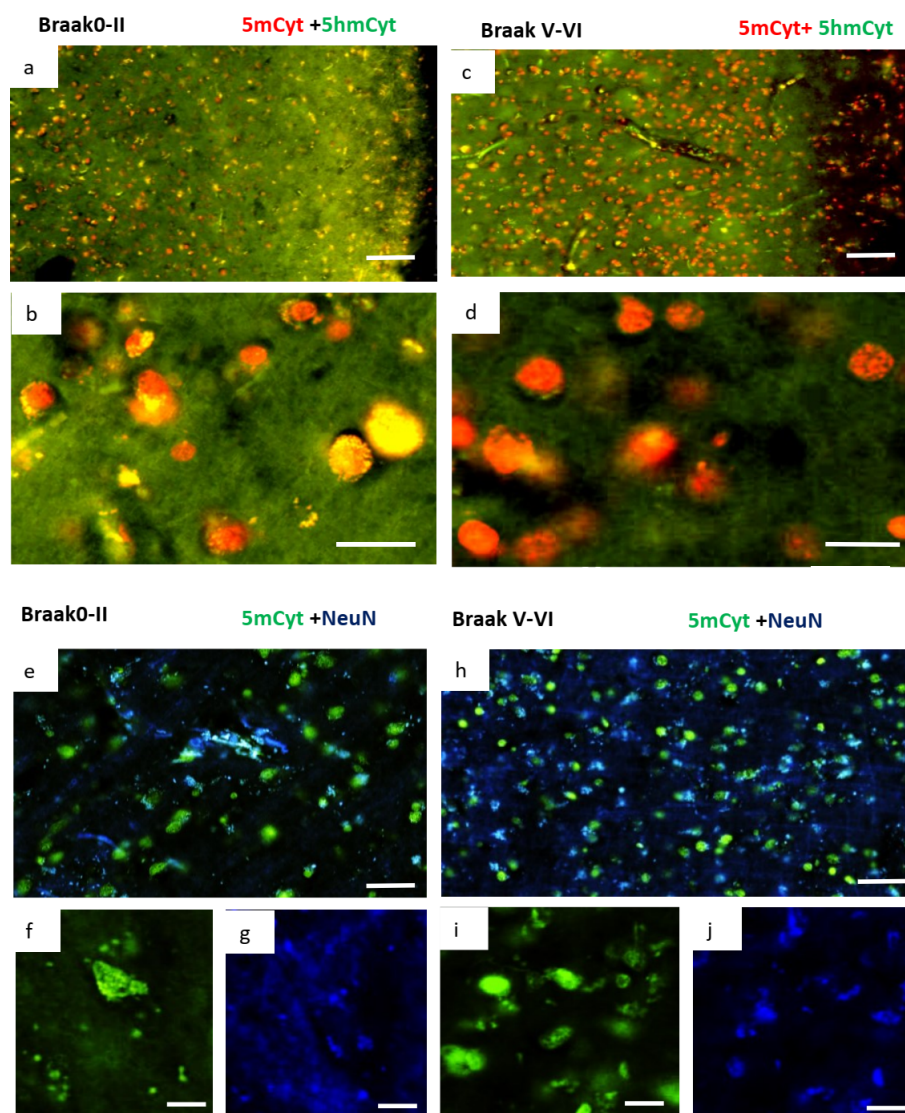


Figure 7. Immunofluorescence staining for 5-methyl cytosine (5mC, marker of methylation) and 5-hydroxy methyl cytosine (5hmC, marker of demethylation) in neurologically normal (Braak 0-II) and AD (Braak V-VI) brains. Double immunofluorescence staining for 5-methyl cytosine (red) and 5-hydroxy methyl cytosine (green) in normal cortical cells ((a) at 100 \times , scale: 100 μ m and (b) 400 \times , scale: 20 μ m) show a balance of methylation and demethylation (seen as colocalised, yellow staining). In AD brain ((c) at 100 \times , scale: 100 μ m and (d) 400 \times , scale: 20 μ m) cells show almost exclusive methylation with very little demethylation. Double immunofluorescence staining for 5mC (green) and the neuronal marker NeuN (blue) in normal (e) and AD (h) are also shown in separated channels (f,g,i,j) to show that many cells have colocalised with many more in AD brain, indicating hypermethylation of neurones in AD. (e,h), at 100 \times , scale: 100 μ m. (f–j) at 200 \times , scale: 50 μ m. The figure is representative of neurologically normal $n = 3$ and AD $n = 4$ brains.

3. Discussion

In the present study, western and dot blot analysis of CSF demonstrate potentially important changes in cerebral folate supply and transport, where a significant decrease in FDH is evident together with a tendency of raised FR α and folate, perhaps reflecting reduced uptake and use, is seen in AD CSF. These results observed in AD are similar to our previous observations in hydrocephalus [19,36,37]. The reduction in FDH is becoming established as a hallmark of CSF drainage insufficiency and may therefore suggest a similar association with CSF drainage capacity, ventricular dilatation and disease severity in AD [29,30,40]. With ventricular enlargement and/or CSF accumulation found as hallmark features of

many conditions including dementia and AD, Autism and Schizophrenia, depression and bipolar [28,29,32,41–63], a cerebral folate issue may also be present as we have found in early stages of hydrocephalus [19]. Indeed, some of these conditions respond to folate treatments [64–72]. Even though Silverberg and colleagues suggest a decrease in CSF output in ageing, they also describe raised CSF pressure and accumulation of fluid in AD [39,73] indicating that CSF drainage may be the most significant factor as is also suggested by the reduced FDH found in this study. AD is not associated with raised intracranial pressure or hydrocephalus but an association between disease severity and ventricular enlargement has been reported and may be an early marker of the development/progression of this condition [50,74,75]. Reduced FDH would eventually result in reduced availability of folate to the brain. We believe these changes in folate related proteins in CSF are physiological changes rather than dilution effects of increased/increasing fluid since other proteins and metabolites remain at normal or above normal levels, e.g., for FR α and folate (other data in preparation for publication).

In the current study, we established how FDH⁺ astrocytes are distributed throughout the adult brain, forming a network stretching from the pia mater of the cerebral cortex to the ventricular zone. Although FDH has been identified as an astrocyte marker, the current study is the first to describe this unique network of cells we believe is involved in folate delivery. Folate supply in the developing brain is from the CSF into FDH⁺ radial glia [19]. As gliogenesis progresses in later development, then several types and forms of astroglia appear throughout the cortex [76] and the radial glia lose their connection to the pia mater to become ependymal cells. As the cortex enlarges, the FDH cells provide essential folate for DNA synthesis, methylation, neurotransmitter and nitric oxide synthesis, myelination as well as other essential metabolic pathways [20]. The normal feeder for this network is FDH in the CSF that binds to folate and FR α and this is required for transport across the ependymal barrier from the ventricles, and the pia mater from the subarachnoid space [19,77]. Where CSF dynamics and drainage are abnormal, FDH is not secreted into the CSF and the brain is deprived of folate through this route as we have found in hydrocephalus. The situation in AD indicates that a similar folate block exists through decreased FDH in the CSF. However, FR α seems able to transport folate into the adult affected brain through a different, perhaps less specific route, the GFAP astrocyte network. In this case, metabolism is also different with hypermethylation occurring in the affected brain regions examined in this study.

A significant finding in normal brain is that the pia mater and marginal zone seem to be essential for folate transfer from CSF into the cortex giving the subarachnoid CSF a vital function in delivering this critical metabolite [77]. In the marginal zone, FDH-positive astrocytes are significantly associated with the main blood vessels entering the brain. These vessels are surrounded by Virchow-Robin spaces which are filled with CSF so that the astrocytes are in contact with the CSF in these compartments most recently associated with the glymphatic pathway [78–80]. Interestingly, these vessels are also the site for glymphatic fluid transfer into the brain parenchyma so that the FDH⁺ astrocytes may be involved in this process as well as other astrocyte functions. FDH⁺ as well as other astrocytes are also associated with the capillary network throughout the brain.

Previous studies have reported that folate is transported across the choroid plexus into the CSF by FR α with little, if any, transport across the endothelial blood–brain barrier [81]. Although positive staining for reduced folate carrier (RFC) in cortical endothelium and neurons has been reported (Human Protein Atlas: <https://www.proteinatlas.org/>, accessed on 7 September 2021) and RFC is elevated in mice missing FR α [81] but this does not seem to happen where FR α is blocked later in life [12,16,66,82]. In our present study, we demonstrated that within normal brain, the FDH⁺/FR α ⁺/GFAP[−]/folate⁺ cells seem to form the main pathway for folate delivery. It seems likely that both FR α and FDH, perhaps bound together by folate, carry folate into the brain through this pathway. Thus, FDH must be synthesised by the cells, secreted into the CSF and then reabsorbed when bound to folate or folate+ FR α .

In the AD brain, an increase in $\text{FR}\alpha^+$ / GFAP^+ /folate⁺ cells indicates that a different pathway opens to $\text{FR}\alpha$ -folate through GFAP-positive astrocytes. An increased expression of $\text{FR}\alpha^+$ / GFAP^+ /folate⁺ cells in the brain of AD is also in line with a decrease in CSF levels of $\text{FR}\alpha$ and folate, though the decrease we found was not significant [81]. Similar to our findings in hydrocephalus, there does seem to be more FDH in the AD brain tissue seen in the density of FDH^+ / GFAP^+ astrocyte processes as well as a greater intensity of staining. This may be a consequence of greater synthesis and expression of FDH by the astrocytes and/or by the inhibition of secretion into the CSF [19,66,72,82–87]. Consequently, a decrease in FDH in AD CSF would have the effect of preventing $\text{FR}\alpha$ uptake into the FDH astrocyte network, leading to the changes we observe in the AD brain. It seems possible that the loss of FDH in the CSF, and associated changes observed in the Alzheimer's brain, may also contribute to glymphatic impairment and the build-up of toxins in the brain including tau and amyloid [80,88–94].

In AD brain, an increase in 5mc indicates enhanced methylation in NeuN^+ neurons and is in line with increased $\text{FR}\alpha^+$ /folate⁺/ NeuN^+ cells that were also associated with the FDH^+ /folate⁺ astrocytes processes indicating enhanced accumulation of $\text{FR}\alpha$ bound folate into the neurons. FDH-bound folate transported in the astrocytes is also feeding the neurons and, as a consequence, neuronal cells are in a state of hypermethylation. The literature on AD brains is contradictory with some finding hypomethylation and some hypermethylation. These differences may reflect the different areas/subareas being analysed and one might speculate that those areas essential for function may be hypomethylated, while those not essential are being shut down by hypermethylation to protect against the neurodegenerative processes in AD. The folate changes we have found need more detailed analysis to establish their roles in cause, aetiology and progression of the disease.

4. Materials and Methods

4.1. Brain Tissue

All brain tissues were supplied from the Manchester Brain Bank under their ethical approval (09/H0906/52+5 and 19/NE/0242) for collection and use of human tissue in neurodegenerative disease research. In this study, we were provided with formalin-fixed tissue from the temporal cortex that included the full thickness of the cortex from the pia mater to the ventricular endymal. Post-mortem CSF samples were also provided from the same brains. Case information is given in Table 1a,b.

Table 1. (a) Normal ageing cases. (b) Alzheimer's disease cases.

(a)								
Case No.	Braak Grade	MRC ID	Gender	Age at Death	Clinical Diagnosis	Pathological Diagnosis 1	Pathological Diagnosis 2	Post Mortem Delay (h)
DPM11/29	II	BBN_3467	M	89	normal	Age changes only	mild SVD	123
DPM13/07	0	BBN_10263	F	Na	normal	leptomeningeal Ca infiltration	Normal	90
DPM14/08	0-I	BBN_20005	M	85	Normal	Age changes only	moderate SVD	98
DPM14/11	I-II	BBN_20195	M	91	Normal	mild SVD	Na	43.5
DPM17/09	I	BBN005.30100	F	88	Control	Normal for age	ARTAG, possible PART	52.5
DPM17/36	I-II	BBN005.32382	F	94	Control	Age changes only	Na	70

Table 1. Cont.

(a)								
Case No.	Braak Grade	MRC ID	Gender	Age at Death	Clinical Diagnosis	Pathological Diagnosis 1	Pathological Diagnosis 2	Post Mortem Delay (h)
DPM18/11	I-II	BBN005.32822	F	90	Control	Age changes only	Possible ARTAG	143
DPM16/29	0-II	BBN005.29063	M	69	Control	Normal for age		53
DPM16/30	0-II	BBN005.29167	F	95	Control	Normal for age/incipient AD	Moderate AD changes in temporal lobe	70.5
DPM16/31	0-II	BBN005.29168	M	90	Control	Normal for age	Mild SVD	155
DPM16/35	0-II	BBN005.29398	M	84	Control	Normal ageing	Mild to moderate SVD	41.5
DPM17/09	0-II	BBN005.30100	F	88	Control	Normal for age	ARTAG, possible PART	52.5
DPM17/23	0-II	BBN005.30844	M	91	Control	Normal for age	Na	88
DPM17/36	0-II	BBN005.32382	F	94	Control	Age changes only	Na	70
DPM17/38	0-II	BBN005.32526	F	101	Control	Normal for age	Na	135.5
DPM16/29	0-I	BBN005.29063	M	69	Control	Normal for age	Na	53
DPM18/03	0-I	BBN005.32560	M	88	Control	Normal for age	Na	39
DPM16/30	0-II	BBN005.29167	F	95	Control	Normal for age/incipient AD	Moderate AD changes in temporal lobe	70.5
DPM16/31	0-II	BBN005.29168	M	90	Control	Normal for age	Mild SVD	155
DPM16/35	0-II	BBN005.29398	M	84	Control	Normal ageing	Mild to moderate SVD	41.5
DPM17/23	0-II	BBN005.30844	M	91	Control	Normal for age	Na	88
DPM14/46	0-I	BBN_24316	F	94	control	age changes only	mild SVD	111
DPM16/30	II	BBN005.29167	F	95	Control	Normal for age/incipient AD	Na	70.5
DPM16/35	II	BBN005.29398	M	84	Control	Normal ageing	Na	41.5
DPM13/07	II	BBN_10263	F	60	normal	leptomeningeal Ca infiltration	Na	90

Table 1. Cont.

(a)								
Case No.	Braak Grade	MRC ID	Gender	Age at Death	Clinical Diagnosis	Pathological Diagnosis 1	Pathological Diagnosis 2	Post Mortem Delay (h)
DPM14/34	0	BBN_24212	F	94	control	age changes only	Na	74.5
(b)								
Case No.	Braak Grade	MRC ID	Gender	Age at Death	Clinical Diagnosis	Pathological Diagnosis 1	Pathological Diagnosis 2	Post Mortem Delay (h)
DPM11/28	VI	BBN_3466	F	71	Alzheimer's disease	Alzheimer's disease		5
DPM12/01	V-VI	BBN_3469	M	67	Dementia	Alzheimer's disease	mild SVD	84
DPM12/03	VI	BBN_3470	M	72	Alzheimer's Disease	Alzheimer's disease	Na	81
DPM12/05	VI	BBN_3472	M	73	Alzheimer's Disease	Alzheimer's disease	mod SVD	5
DPM12/25	V-VI	BBN_6076	M	62	Semantic Dementia	Alzheimer's disease	Na	50.5
DPM12/32	V-VI	BBN_9480	M	73	Alzheimer's disease	Alzheimer's disease	Na	26
DPM13/10	V-VI	BBN_11028	F	85	dementia	Alzheimer's disease	Mild CAA	24
DPM14/10	V-VI	BBN_20007	F	78	Alzheimer's disease	Alzheimer's disease	CAA with capillary involvement	70
DPM14/30	V-VI	BBN_23794	F	70	dementia, learning difficulty	Alzheimer's disease	Na	89
DPM14/31	VI	BBN_23803	M	64	Alzheimer's Disease	Alzheimer's disease	moderate SVD	98.5
DPM14/50	V-VI	BBN_24361	F	63	Alzheimer's Disease	Alzheimer's disease	moderate SVD	54
DPM15/02	V-VI	BBN_24373	M	78	Alzheimer's Disease	Alzheimer's disease	sec TDP-43 proteinopathy	173
DPM15/29	V-VI	BBN_25921	M	81	AD and Vascular dementia	Alzheimer's disease	mild SVD	68
DPM16/10	V-VI	BBN005.28400	F	59	Alzheimer's Disease	Alzheimer's disease	Na	87
DPM18/27	V-VI	BBN005.33712	M	75	Alzheimer's Disease	Alzheimer's disease	Na	104.5
DPM16/40	VI	BBN005.29461	M	82	Alzheimer's Disease	Alzheimer's disease	Moderate CAA	25.5
DPM17/37	V-VI	BBN005.32384	F	90	Alzheimer's Disease	Alzheimer's disease	Possible AGD	76
DPM18/12	VI	BBN005.32823	M	70	Alzheimer's Disease	Alzheimer's disease	Moderate SVD	120.5

Table 1. Cont.

(b)								
Case No.	Braak Grade	MRC ID	Gender	Age at Death	Clinical Diagnosis	Pathological Diagnosis 1	Pathological Diagnosis 2	Post Mortem Delay (h)
DPM18/39	VI	BBN005.35131	F	75	Dementia	Alzheimer's disease	Na	127.5
DPM19/04	VI	BBN005.35211	M	82	Alzheimer's Disease	Alzheimer's disease	Temporal intra-cortical infarct. Secondary TDP-43.	124
DPM19/07	VI	BBN005.35399	F	86	Dementia	Alzheimer's disease	Severe hippocampal sclerosis. Secondary TDP-43.	72
DPM20/07	VI	BBN005.36133	F	88	Alzheimer's Disease	Alzheimer's disease	Na	165.5
DPM10/15	VI	BBN_5766	F	76	Alzheimer's disease	Alzheimer's disease	Na	52
DPM14/10	V-VI	BBN_20007	F	78	Alzheimer's disease	Alzheimer's disease	Na	70
DPM11/28	VI	BBN_3466	F	71	Alzheimer's disease	Alzheimer's disease	Na	64
DPM12/03	VI	BBN_3470	M	72	Alzheimer's Disease	Alzheimer's disease	Na	81
DPM12/17	VI	BBN_6068	M	76	Alzheimer's Disease	Alzheimer's disease	Na	96
DPM14/31	VI	BBN_23803	M	64	Alzheimer's Disease	Alzheimer's disease	Na	98.5
DPM12/01	V-VI	BBN_3469	M	67	Dementia	Alzheimer's disease	Na	84
DPM14/21	IV	BBN_21006	M	72	FTD	Alzheimer's disease	Na	103
DPM13/30	IV	BBN_15257	M	77	FTD/PNFA	Alzheimer's disease	Na	87

Only individuals who were neuropathologically normal (Braak 0-II, $n = 21$), based on clinical observation and post-mortem neuropathology assessment, or with severe AD (Braak V-VI, $n = 21$) were included in this small cohort study. Due to these selection criteria, there was significant variability in post-mortem times to collection of tissue (Table 1). The CSF from all cases was analysed but for tissue analysis and immunohistochemistry we used 3 cases from neurologically normal and 4 from severe AD (highlighted in bold text in Table). A full analysis of clinic-pathological features for these patients has been published in our previous report [20]. In a study addressing the issues of post-mortem delay (PMD) to the quality of brain tissue samples, Robinson et al. [73] refute the view that extended PMD is detrimental to brain tissue quality. The paper indicates that this is determined by brain pH and that pH is not significantly affected by post-mortem time.

4.2. Western and Dot Blots

For relative measures of CSF proteins, western blot analysis of CSF was performed comparing normal ($n = 21$) and AD ($n = 21$). Samples were prepared by mixing 6 μ L of CSF with Laemmli sample buffer (Bio-Rad Labs Ltd., Watford, UK) and 2-mercaptoethanol (Sigma-Aldrich, Gillingham, UK) then heated to 70 °C for 10 min before cooling and loading into Nupage precast SDS polyacrylamide gels (Life Technologies, Paisley, UK). 150 v were applied to the gels to separate the proteins over a 40–60 min run. Proteins were transferred onto nitrocellulose membranes using an iBlot semi-dry transfer system (Life Technologies,

Paisley, UK). Blots were then placed in a blocking buffer (5% BSA in PBS with 1% tween 20) for an hour before being probed with a primary antibody to the specific protein of interest (Table 2) in the same blocking buffer, at a common dilution of 1:3000, overnight at 4 °C. Blots were washed in PBS with 0.1% tween 20 and then incubated in secondary antibody conjugated to HRP for 2 h at room temperature before a further wash. Membranes were then incubated in ECL solution (Bio-Rad Labs Ltd., Watford, UK) for 5 min before exposure on a LiCor C-digit scanner (Li-Cor Biotechnology Ltd., Cambridge, UK). Scans were collected into LiCor Image Studio software for quantification and analysis. For dot blots, 6 µL of CSF from normal ($n = 21$) and AD ($n = 21$), were placed directed on nitrocellulose membranes and allowed to spread and dry at room temperature for an hour. They were then blocked, and the remaining procedure was as described for Western blots. All antibodies used in this study are listed in Table 2.

Table 2. Antibodies used in this study.

Target	Primary Antibodies			Dilution		
	Species	Source	Ref. No	WB	DB	IHC
FDH	Rb anti Human	S.Krupenko	Gift	—	—	1:1000
FDH	Ms-anti-ALDH1L1	Sigma	SAB 4100141	—	—	1:1000
FR α	Gt-anti-FOLR1	R & D System	AF5646	1:3000	—	1:1000
Folates	Ms anti Human	Sigma	M-5028	—	—	—
GFAP	Chkn-anti-GFAP	Encor	CPCA-GFAP	—	—	1:3000
S100	Rb-anti-S100	Atlas Ab	HPA015768	—	—	1:1000
5-HmCyt	Rat-anti-5-HmCyt	Abcam	Ab106918	—	—	1:1000
5-mCyt	Rb-anti-5mCyt	Cell Signalling	D3S2Z	—	—	1:1000
Fluorophore-Conjugated Secondary Antibodies for WB/DB				Dilutions		
Species		Source	Ref. No	WB	DB	
anti Rb		Bio-Rad	10000068188D	1:3000	—	
anti Ms		Bio-Rad	10000086250B	1:3000	1:3000	
Alexa Fluor Secondary Antibodies for IHC				Dilutions		
Species		Source	Ref. No	wavelength	IHC	
Anti-Chkn		Abcam	ab150176	594	1:3000	
Anti-Rb		Abcam	ab150077	488	1:1000	
Anti-Ms		Abcam	ab150120	594	1:1000	
Anti-Gt		Abcam	ab150132	594	1:1000	
Anti-Ms		Abcam	ab150113	488	1:1000	
Anti-Chkn		Abcam	ab150169	488	1:3000	
Anti-Rat		Abcam	ab150165	488	1:1000	
Anti-Rb		Abcam	ab150080	594	1:1000	
Anti-Rb		Abcam	ab150075	647	1:1000	
Anti-Gt		Abcam	ab150129	488	1:1000	
Anti-Ms		Abcam	ab150110	555	1:1000	

4.3. Immunohistochemistry

The formalin-fixed superior and medial temporal gyrus from subjects with definite AD ($n = 4$) and normal subjects showing mild ageing-related changes ($n = 3$) were obtained from the Manchester Brain Bank. The samples included the arachnoid, cortex, white matter and ventricular wall. The tissue specimens were washed and incubated in 30% sucrose solution (for cryoprotection) for several days until they sank. They were then frozen in isopentane cooled with dry ice before mounting on a stub and locating into the chuck of a Leica DM1900 cryostat (Leica Microsystems Ltd., Milton Keynes, UK). 50 μm thick sections were obtained which spanned from pia mater to the ependyma. Sections were collected as free-floating rather than onto glass slides to ensure optimal immuno staining. Heat-induced epitope retrieval was performed in pre-heated sodium citrate buffer (pH 6.0) microwaved for 5–10 s and kept in the cooling solution for half an hour. Sections were then incubated in blocking buffer, consisting of 1% Triton-X100 (Sigma-Aldrich, Gillingham, UK) in Phosphate-buffered saline (PBS) containing 0.5% goat serum and 0.5% donkey serum, and then incubated in primary antibodies (listed in Table 2) diluted in the same blocking buffer overnight at 4 °C. Washing in PBS with 1% Tween-20 (Sigma-Aldrich, Gillingham, UK) was followed by incubation in Alexa Fluor conjugated secondary antibodies (Table 2) in the same solution. After further buffer washes to remove unbound antibodies, the sections were placed onto glass slides and mounted in Fluoroshield (Abcam, Cambridge, UK) containing 4',6-diamidino-2-phenylindole (DAPI) to stain nuclei. Coverslips were sealed around the edges with clear nail varnish to prevent movement during scanning. Sections were scanned on a 3D Histech Panoramic 250 Flash Slide Scanner (3DHistech Ltd., Budapest, Hungary) before viewing on 3D Histech Caseviewer software.

4.4. Statistical Analysis

Adjusted band volume and dot volume intensities were obtained using ImageLab software by subtracting the background intensity for each blot image from the band or dot volume of each individual. Adjusted band volume was averaged across repeat experiments and presented in arbitrary units of optical density (OD). GraphPad Prism Version 9.2.0 was used to analyse the differences between average adjusted band volumes of normal compared to AD. Normality tests were not required due to the small number of individuals in each group, thus parametric tests were robust enough in this circumstance. All groups were tested for equal variance with an F test. Data sets with equal variance were analysed using a Student's unpaired *t*-test. Those that failed to show equal variance had a Welch correction applied to this *t*-test. All data were presented as mean \pm standard error of the mean (\pm SEM) and to 4 decimal places. Statistical significance was expressed at the $p < 0.05$ level throughout.

5. Conclusions

The current study has identified a potentially important change in folate supply to the AD brain. We postulate that with a decrease in the folate binding protein, FDH in the CSF, there is a switch in folate supply from the FR α -FDH pathway to the FR α -GFAP pathway. The consequence of this switch seems to be a change in metabolism to hypermethylation where FR α , with folate, ends up in the neurons of the cortex and the folate is delivered to the nuclei where methylation occurs. We further suggest that this may be a strategy to shut down all but essential activity to safeguard surviving neurons from the toxic effects of AD. This may in turn explain some of the cognitive decline not attributable to the loss of neurons alone. These findings present strong evidence for a larger and more detailed study of cerebral folate metabolism in AD.

Limitations of the Current Study

The biggest limitation of this study was in the use of post-mortem tissues and matched post-mortem CSF samples. In addition, we only included 21 individuals in each group for CSF analysis and only 4 AD and 3 normal in the immunohistochemistry experiments.

Although the variable post-mortem time, would perhaps, not produce consistent results and may explain some of the variability we observed although published evidence suggests this should not be a significant issue [73]. Table 1 indicates the range in post-mortem times that were a consequence of the selection criteria for the study in terms of severity of AD. We wished to compare clearly neurologically normal brains to the most severe cases of AD within the Brain Bank to establish whether an effect existed or not. The immunohistochemical data is reported in a descriptive way due to the small number analysed.

Supplementary Materials: The supporting information can be downloaded at: <https://www.mdpi.com/article/10.3390/ijms24010660/s1>.

Author Contributions: J.A.M. conceived the project and supervised all aspects of the research including analysis of data and writing the original manuscript. S.F.N., N.H., K.W. and P.L. carried out laboratory experiments. N.N. revised the manuscript following reviewer comments, carrying out additional immunohistochemical and western/dot blot experiments and analyses. F.R. and A.C.R. provided brain tissues, carried out neuropathology examinations to grade each brain, and edited the manuscript. All authors have read and agreed to the published version of the manuscript.

Funding: This study was funded by The Charles Wolfson Charitable Trust and The African Healthcare Development Trust (JAM) and by the Commonwealth Scholarship Commission (SFN).

Institutional Review Board Statement: Study performed under Manchester Brain Bank ethical approval for human tissue use in ageing studies.

Data Availability Statement: All data are available from the corresponding author.

Acknowledgments: We thank the Bioscience Imaging Core Facility staff for help in imaging. Tissue samples were supplied by The Manchester Brain Bank, which is part of the Brains for Dementia Research Initiative, jointly funded by Alzheimer's Society and Alzheimer's Research UK.

Conflicts of Interest: The authors declare no conflict of interest in this publication.

Abbreviations

AD	Alzheimer's disease
FOLR1 and FR α	folate receptor alpha
ALDH1L1 and FDH	10-formyl tetrahydrofolate dehydrogenase
MTR	methionine synthase with full name: 5-methyltetrahydrofolate-homocysteine methyltransferase
MTRR	methionine synthase reductase, full name: methionine synthase-cobalamin methyltransferase
MTHFD1	methylene tetrahydrofolate dehydrogenase 1
DHFR	dihydrofolate reductase
MTHFR	methylene tetrahydrofolate reductase
5mTHF	5 methyl tetrahydrofolate
GFAP	glial fibrillary acidic protein
5mCyt	5 methyl cytosine
5HmCyt	5 hydroxy methyl cytosine

References

1. Ferri, C.P.; Prince, M.; Brayne, C.; Brodaty, H.; Fratiglioni, L.; Ganguli, M.; Hall, K.; Hasegawa, K.; Hendrie, H.; Huang, Y.; et al. Global prevalence of dementia: A Delphi consensus study. *Lancet* **2005**, *366*, 2112–2117. [[CrossRef](#)] [[PubMed](#)]
2. Liu, P.-P.; Xie, Y.; Meng, X.-Y.; Kang, J.-S. History and progress of hypotheses and clinical trials for Alzheimer's disease. *Signal Transduct. Target. Ther.* **2019**, *4*, 1–22. [[CrossRef](#)] [[PubMed](#)]
3. Oberman, K.; Gouweleeuw, L.; Hoogerhout, P.; Eisel, U.L.; van Riet, E.; Schoemaker, R.G. Vaccination Prevented Short-Term Memory Loss, but Deteriorated Long-Term Spatial Memory in Alzheimer's Disease Mice, Independent of Amyloid-beta Pathology. *J. Alzheimer's Dis. Rep.* **2020**, *4*, 261–280. [[CrossRef](#)] [[PubMed](#)]
4. Mantile, F.; Prisco, A. Vaccination against β -Amyloid as a Strategy for the Prevention of Alzheimer's Disease. *Biology* **2020**, *9*, 425. [[CrossRef](#)]

5. Stoiljkovic, M.; Horvath, T.L.; Hajós, M. Therapy for Alzheimer's disease: Missing targets and functional markers? *Ageing Res. Rev.* **2021**, *68*, 101318. [[CrossRef](#)]
6. Steinfeld, R.; Grapp, M.; Kraetzner, R.; Dreha-Kulaczewski, S.; Helms, G.; Dechent, P.; Wevers, R.; Grosso, S.; Gärtner, J. Folate Receptor Alpha Defect Causes Cerebral Folate Transport Deficiency: A Treatable Neurodegenerative Disorder Associated with Disturbed Myelin Metabolism. *Am. J. Hum. Genet.* **2009**, *85*, 354–363. [[CrossRef](#)]
7. Krupenko, S.A.; Krupenko, N.I. Loss of ALDH1L1 folate enzyme confers a selective metabolic advantage for tumor progression. *Chem. Interact.* **2019**, *302*, 149–155. [[CrossRef](#)]
8. Krupenko, S.A.; Krupenko, N.I. ALDH1L1 and ALDH1L2 Folate Regulatory Enzymes in Cancer. *Adv. Exp. Med. Biol.* **2018**, *1032*, 127–143. [[CrossRef](#)]
9. Krupenko, S.A.; Horita, D.A. The Role of Single-Nucleotide Polymorphisms in the Function of Candidate Tumor Suppressor ALDH1L1. *Front. Genet.* **2019**, *10*, 1013. [[CrossRef](#)]
10. Oleinik, N.V.; Krupenko, N.; A Krupenko, S. ALDH1L1 inhibits cell motility via dephosphorylation of cofilin by PP1 and PP2A. *Oncogene* **2010**, *29*, 6233–6244. [[CrossRef](#)]
11. Ramaekers, V.; Segers, K.; Sequeira, J.; Koenig, M.; Van Maldergem, L.; Bours, V.; Kornak, U.; Quadros, E. Genetic assessment and folate receptor autoantibodies in infantile-onset cerebral folate deficiency (CFD) syndrome. *Mol. Genet. Metab.* **2018**, *124*, 87–93. [[CrossRef](#)] [[PubMed](#)]
12. Ramaekers, V.T.; Quadros, E.V.; Sequeira, J.M. Role of folate receptor autoantibodies in infantile autism. *Mol. Psychiatry* **2012**, *18*, 270–271. [[CrossRef](#)] [[PubMed](#)]
13. Hasselmann, O.; Blau, N.; Ramaekers, V.T.; Quadros, E.V.; Sequeira, J.; Weissert, M. Cerebral folate deficiency and CNS inflammatory markers in Alpers disease. *Mol. Genet. Metab.* **2010**, *99*, 58–61. [[CrossRef](#)]
14. Bonkowsky, J.L.; Ramaekers, V.T.; Quadros, E.V.; Lloyd, M. Progressive encephalopathy in a child with cerebral folate deficiency syndrome. *J. Child Neurol.* **2008**, *23*, 1460–1463. [[CrossRef](#)] [[PubMed](#)]
15. Ramaekers, V.T.; Blau, N.; Sequeira, J.M.; Nassogne, M.-C.; Quadros, E.V. Folate Receptor Autoimmunity and Cerebral Folate Deficiency in Low-Functioning Autism with Neurological Deficits. *Neuropediatrics* **2007**, *38*, 276–281. [[CrossRef](#)]
16. Ramaekers, V.T.; Rothenberg, S.P.; Sequeira, J.M.; Opladen, T.; Blau, N.; Quadros, E.V.; Selhub, J. Autoantibodies to Folate Receptors in the Cerebral Folate Deficiency Syndrome. *N. Engl. J. Med.* **2005**, *352*, 1985–1991. [[CrossRef](#)]
17. Frye, R.E.; Delhey, L.; Slattery, J.; Tippett, M.; Wynne, R.; Rose, S.; Kahler, S.G.; Bennuri, S.C.; Melnyk, S.; Sequeira, J.M.; et al. Blocking and Binding Folate Receptor Alpha Autoantibodies Identify Novel Autism Spectrum Disorder Subgroups. *Front. Neurosci.* **2016**, *10*, 80. [[CrossRef](#)]
18. Frye, R.E.; Sequeira, J.M.; Quadros, E.V.; James, S.J.; Rossignol, D.A. Cerebral folate receptor autoantibodies in autism spectrum disorder. *Mol. Psychiatry* **2013**, *18*, 369–381. [[CrossRef](#)]
19. Cains, S.; Shepherd, A.; Nabiuni, M.; Owen-Lynch, P.J.; Miyani, J. Addressing a Folate Imbalance in Fetal Cerebrospinal Fluid Can Decrease the Incidence of Congenital Hydrocephalus. *J. Neuropathol. Exp. Neurol.* **2009**, *68*, 404–416. [[CrossRef](#)]
20. Miyani, J.; Buttercase, C.; Beswick, E.; Miyani, S.; Moshkdanian, G.; Naz, N. Folate Related Pathway Gene Analysis Reveals a Novel Metabolic Variant Associated with Alzheimer's Disease with a Change in Metabolic Profile. *Metabolites* **2022**, *12*, 475. [[CrossRef](#)]
21. Silverberg, G.D. The cerebrospinal fluid production rate is reduced in dementia of the Alzheimer's type. *Neurology* **2001**, *57*, 1763–1766. [[CrossRef](#)] [[PubMed](#)]
22. Silverberg, G.; Mayo, M.; Saul, T.; Fellmann, J.; McGuire, D. Elevated cerebrospinal fluid pressure in patients with Alzheimer's disease. *Cereb. Fluid Res.* **2006**, *3*, 7. [[CrossRef](#)]
23. Ott, B.R.; Cohen, R.A.; Gongvatana, A.; Okonkwo, O.C.; Johanson, C.E.; Stopa, E.G.; Donahue, J.E.; Silverberg, G.D. Brain Ventricular Volume and Cerebrospinal Fluid Biomarkers of Alzheimer's Disease. *J. Alzheimer's Dis.* **2010**, *20*, 647–657. [[CrossRef](#)] [[PubMed](#)]
24. Chiu, C.; Miller, M.C.; Caralopoulos, I.N.; Worden, M.S.; Brinker, T.; Gordon, Z.N.; Johanson, C.; Silverberg, G.D. Temporal course of cerebrospinal fluid dynamics and amyloid accumulation in the aging rat brain from three to thirty months. *Fluids Barriers CNS* **2012**, *9*, 3. [[CrossRef](#)] [[PubMed](#)]
25. Shen, M.D. Cerebrospinal fluid and the early brain development of autism. *J. Neurodev. Disord.* **2018**, *10*, 39. [[CrossRef](#)]
26. Shen, M.D.; Nordahl, C.W.; Li, D.D.; Lee, A.; Angkustsiri, K.; Emerson, R.W.; Rogers, S.J.; Ozonoff, S.; Amaral, D.G. Extra-axial cerebrospinal fluid in high-risk and normal-risk children with autism aged 2–4 years: A case-control study. *Lancet Psychiatry* **2018**, *5*, 895–904. [[CrossRef](#)]
27. Shen, M.D.; Kim, S.H.; McKinstry, R.C.; Gu, H.; Hazlett, H.C.; Nordahl, C.W.; Emerson, R.W.; Shaw, D.; Elison, J.T.; Swanson, M.R.; et al. Increased Extra-axial Cerebrospinal Fluid in High-Risk Infants Who Later Develop Autism. *Biol. Psychiatry* **2017**, *82*, 186–193. [[CrossRef](#)]
28. Movsas, T.Z.; Pinto-Martin, J.A.; Whitaker, A.H.; Feldman, J.F.; Lorenz, J.M.; Korzeniewski, S.J.; Levy, S.E.; Paneth, N. Autism Spectrum Disorder Is Associated with Ventricular Enlargement in a Low Birth Weight Population. *J. Pediatr.* **2013**, *163*, 73–78. [[CrossRef](#)]
29. Nestor, S.M.; Rupsingh, R.; Borrie, M.; Smith, M.; Accomazzi, V.; Wells, J.L.; Fogarty, J.; Bartha, R.; Initiative, T.A.D.N. Ventricular enlargement as a possible measure of Alzheimer's disease progression validated using the Alzheimer's disease neuroimaging initiative database. *Brain* **2008**, *131*, 2443–2454. [[CrossRef](#)]

30. Chou, Y.-Y.; Leporé, N.; Avedissian, C.; Madsen, S.K.; Parikshak, N.; Hua, X.; Shaw, L.M.; Trojanowski, J.Q.; Weiner, M.W.; Toga, A.W.; et al. Mapping correlations between ventricular expansion and CSF amyloid and tau biomarkers in 240 subjects with Alzheimer's disease, mild cognitive impairment and elderly controls. *Neuroimage* **2009**, *46*, 394–410. [[CrossRef](#)]
31. Madsen, S.K.; (Adni), F.T.A.D.N.I.; Gutman, B.A.; Joshi, S.H.; Toga, A.W.; Jack, C.R.; Weiner, M.W.; Thompson, P.M. Mapping Dynamic Changes in Ventricular Volume onto Baseline Cortical Surfaces in Normal Aging, MCI, and Alzheimer's Disease. *Multimodal. Brain Image Anal.* **2013**, *8159*, 84–94. [[CrossRef](#)]
32. Ye, B.S.; Lee, Y.; Kwak, K.; Park, Y.-H.; Ham, J.H.; Lee, J.J.; Shin, N.-Y.; Lee, J.-M.; Sohn, Y.H.; Lee, P.H. Posterior Ventricular Enlargement to Differentiate Dementia with Lewy Bodies from Alzheimer's Disease. *J. Alzheimer's Dis.* **2016**, *52*, 1237–1243. [[CrossRef](#)]
33. Mahajan, U.V.; Varma, V.R.; Griswold, M.E.; Blackshear, C.T.; An, Y.; Oommen, A.M.; Varma, S.; Troncoso, J.C.; Pletnikova, O.; O'Brien, R.; et al. Dysregulation of multiple metabolic networks related to brain transmethylation and polyamine pathways in Alzheimer disease: A targeted metabolomic and transcriptomic study. *PLoS Med.* **2020**, *17*, e1003012. [[CrossRef](#)]
34. Cao, X.; Wolf, A.; Kim, S.-E.; Cabrera, R.M.; Wlodarczyk, B.J.; Zhu, H.; Parker, M.; Lin, Y.; Steele, J.W.; Han, X.; et al. *CIC de novo* loss of function variants contribute to cerebral folate deficiency by downregulating *FOLR1* expression. *J. Med. Genet.* **2020**, *58*, 484–494. [[CrossRef](#)]
35. Grapp, M.; Wrede, A.; Schweizer, M.; Hüwel, S.; Galla, H.-J.; Snaidero, N.; Simons, M.; Bückers, J.; Low, P.S.; Urlaub, H.; et al. Choroid plexus transcytosis and exosome shuttling deliver folate into brain parenchyma. *Nat. Commun.* **2013**, *4*, 2123. [[CrossRef](#)]
36. Jimenez, A.R.; Naz, N.; Miyan, J. Altered folate binding protein expression and folate delivery are associated with congenital hydrocephalus in the hydrocephalic Texas rat. *J. Cereb. Blood Flow Metab.* **2018**, *39*, 2061–2073. [[CrossRef](#)]
37. Naz, N.; Jimenez, A.R.; Sanjuan-Vilaplana, A.; Gurney, M.; Miyan, J. Neonatal hydrocephalus is a result of a block in folate handling and metabolism involving 10-formyltetrahydrofolate dehydrogenase. *J. Neurochem.* **2016**, *138*, 610–623. [[CrossRef](#)]
38. Mashayekhi, F.; Draper, C.E.; Bannister, C.M.; Pourghasem, M.; Owen-Lynch, P.J.; Miyan, J.A. Deficient cortical development in the hydrocephalic Texas (H-Tx) rat: A role for CSF. *Brain* **2002**, *125*, 1859–1874. [[CrossRef](#)]
39. Owen-Lynch, P.J.; Draper, C.E.; Mashayekhi, F.; Bannister, C.M.; Miyan, J.A. Defective cell cycle control underlies abnormal cortical development in the hydrocephalic Texas rat. *Brain* **2003**, *126*, 623–631. [[CrossRef](#)]
40. Coupé, P.; Manjón, J.V.; Lanuza, E.; Catheline, G. Lifespan Changes of the Human Brain in Alzheimer's Disease. *Sci. Rep.* **2019**, *9*, 1–12. [[CrossRef](#)]
41. Saijo, T.; Abe, T.; Someya, Y.; Sassa, T.; Sudo, Y.; Suhara, T.; Shuno, T.; Asai, K.; Okubo, Y. Ten year progressive ventricular enlargement in schizophrenia: An MRI morphometrical study. *Psychiatry Clin. Neurosci.* **2001**, *55*, 41–47. [[CrossRef](#)] [[PubMed](#)]
42. Jericó, D.; Luis, E.; Cussó, L.; Fernández-Seara, M.; Morales, X.; Córdoba, K.M.; Benito, M.; Sampedro, A.; Larriva-Hormigos, M.; Ramírez, M.J.; et al. Brain ventricular enlargement in human and murine acute intermittent porphyria. *Hum. Mol. Genet.* **2020**, *29*, 3211–3223. [[CrossRef](#)] [[PubMed](#)]
43. Goukasian, N.; Porat, S.; Blanken, A.; Avila, D.; Zlatev, D.; Hurtz, S.; Hwang, K.S.; Pierce, J.; Joshi, S.H.; Woo, E.; et al. Cognitive Correlates of Hippocampal Atrophy and Ventricular Enlargement in Adults with or without Mild Cognitive Impairment. *Dement. Geriatr. Cogn. Disord. Extra* **2019**, *9*, 281–293. [[CrossRef](#)] [[PubMed](#)]
44. Zhao, H.; Wei, T.; Li, X.; Ba, T. Early life adversity induced third ventricular enlargement in young adult male patients suffered from major depressive disorder: A study of brain morphology. *Folia Morphol.* **2018**, *77*, 428–433. [[CrossRef](#)]
45. Mak, E.; Su, L.; Williams, G.B.; Firbank, M.J.; Lawson, R.A.; Yarnall, A.J.; Duncan, G.W.; Mollenhauer, B.; Owen, A.M.; Khoo, T.K.; et al. Longitudinal whole-brain atrophy and ventricular enlargement in nondemented Parkinson's disease. *Neurobiol. Aging* **2017**, *55*, 78–90. [[CrossRef](#)]
46. Schenning, K.J.; Murchison, C.F.; Mattek, N.C.; Silbert, L.C.; Kaye, J.A.; Quinn, J.F. Surgery is associated with ventricular enlargement as well as cognitive and functional decline. *Alzheimer's Dement.* **2015**, *12*, 590–597. [[CrossRef](#)]
47. Müller, M.; Esser, R.; Kötter, K.; Voss, J.; Müller, A.; Stellmes, P. Third ventricular enlargement in early stages of multiple sclerosis is a predictor of motor and neuropsychological deficits: A cross-sectional study. *BMJ Open* **2013**, *3*, e003582. [[CrossRef](#)]
48. Sayo, A.; Jennings, R.G.; Van Horn, J.D. Study factors influencing ventricular enlargement in schizophrenia: A 20year follow-up meta-analysis. *NeuroImage* **2012**, *59*, 154–167. [[CrossRef](#)]
49. Apostolova, L.G.; Green, A.E.; Babakchanian, S.; Hwang, K.S.; Chou, Y.-Y.; Toga, A.W.; Thompson, P. Hippocampal Atrophy and Ventricular Enlargement in Normal Aging, Mild Cognitive Impairment (MCI), and Alzheimer Disease. *Alzheimer Dis. Assoc. Disord.* **2012**, *26*, 17–27. [[CrossRef](#)]
50. Jackson, D.C.; Irwin, W.; Dabbs, K.; Lin, J.J.; Jones, J.E.; Hsu, D.A.; Stafstrom, C.E.; Seidenberg, M.; Hermann, B.P. Ventricular enlargement in new-onset pediatric epilepsies. *Epilepsia* **2011**, *52*, 2225–2232. [[CrossRef](#)]
51. Dalaker, T.O.; Zivadinov, R.; Ramasamy, D.P.; Beyer, M.K.; Alves, G.; Bronnick, K.S.; Tysnes, O.-B.; Aarsland, D.; Larsen, J.P. Ventricular enlargement and mild cognitive impairment in early Parkinson's disease. *Mov. Disord.* **2010**, *26*, 297–301. [[CrossRef](#)]
52. Kempton, M.J.; Stahl, D.; Williams, S.C.; DeLisi, L.E. Progressive lateral ventricular enlargement in schizophrenia: A meta-analysis of longitudinal MRI studies. *Schizophr. Res.* **2010**, *120*, 54–62. [[CrossRef](#)]
53. Martola, J.; Stawiarz, L.; Fredrikson, S.; Hillert, J.; Bergström, J.; Flodmark, O.; Aspelin, P.; Wiberg, M.K. Rate of ventricular enlargement in multiple sclerosis: A nine-year magnetic resonance imaging follow-up study. *Acta Radiol.* **2008**, *49*, 570–579. [[CrossRef](#)]

54. Guptha, S.H.; Holroyd, E.; Campbell, G. Progressive lateral ventricular enlargement as a clue to Alzheimer's disease. *Lancet* **2002**, *359*, 2040. [[CrossRef](#)]
55. Vita, A.; Dieci, M.; Silenzi, C.; Tenconi, F.; Giobbio, G.M.; Invernizzi, G. Cerebral ventricular enlargement as a generalized feature of schizophrenia: A distribution analysis on 502 subjects. *Schizophr. Res.* **2000**, *44*, 25–34. [[CrossRef](#)]
56. Elkis, H.; Friedman, L.; Wise, A.; Meltzer, H.Y. Meta-analyses of studies of ventricular enlargement and cortical sulcal prominence in mood disorders. Comparisons with controls or patients with schizophrenia. *Arch. Gen. Psychiatry* **1995**, *52*, 735–746. [[CrossRef](#)]
57. Wang, G.J.; Volkow, N.D.; Roque, C.T.; Cestaro, V.L.; Hitzemann, R.J.; Cantos, E.L.; Levy, A.V.; Dhawan, A.P. Functional importance of ventricular enlargement and cortical atrophy in healthy subjects and alcoholics as assessed with PET, MR imaging, and neuropsychologic testing. *Radiology* **1993**, *186*, 59–65. [[CrossRef](#)]
58. Erel, O.; Cannon, T.D.; Hollister, J.M.; Mednick, S.A.; Parnas, J. Ventricular enlargement and premorbid deficits in school-occupational attainment in a high risk sample. *Schizophr. Res.* **1991**, *4*, 49–52. [[CrossRef](#)]
59. Jakobsen, J.; Gyldensted, C.; Brun, B.; Bruhn, P.; Helweg-Larsen, S.; Arlien-Søborg, P. Cerebral ventricular enlargement relates to neuropsychological measures in unselected AIDS patients. *Acta Neurol. Scand.* **1989**, *79*, 59–62. [[CrossRef](#)]
60. Luxenberg, J.S.; Haxby, J.V.; Creasey, H.; Sundaram, M.; Rapoport, S.I. Rate of ventricular enlargement in dementia of the Alzheimer type correlates with rate of neuropsychological deterioration. *Neurology* **1987**, *37*, 1135. [[CrossRef](#)]
61. Scott, M.L.; Golden, C.J.; Ruedrich, S.L.; Bishop, R.J. Ventricular enlargement in major depression. *Psychiatry Res.* **1983**, *8*, 91–93. [[CrossRef](#)]
62. Nasrallah, H.A.; McCalley-Whitters, M.; Jacoby, C.G. Cerebral ventricular enlargement in young manic males: A controlled CT study. *J. Affect. Disord.* **1982**, *4*, 15–19. [[CrossRef](#)] [[PubMed](#)]
63. Hubbard, B.M.; Anderson, J.M. Age, senile dementia and ventricular enlargement. *J. Neurol. Neurosurg. Psychiatry* **1981**, *44*, 631–635. [[CrossRef](#)] [[PubMed](#)]
64. Frye, R.E.; Slattery, J.; Delhey, L.; Furgerson, B.; Strickland, T.; Tippett, M.; Sailey, A.; Wynne, R.; Rose, S.; Melnyk, S.; et al. Folinic acid improves verbal communication in children with autism and language impairment: A randomized double-blind placebo-controlled trial. *Mol. Psychiatry* **2018**, *23*, 247–256. [[CrossRef](#)] [[PubMed](#)]
65. Ferreira, P.; Luco, S.M.; Sawyer, S.L.; Davila, J.; Boycott, K.M.; Dymont, D.A. Late diagnosis of cerebral folate deficiency: Fewer seizures with folinic acid in adult siblings. *Neurol. Genet.* **2015**, *2*, e38. [[CrossRef](#)]
66. Ramaekers, V.; Thöny, B.; Sequeira, J.; Anseau, M.; Philippe, P.; Boemer, F.; Bours, V.; Quadros, E. Folinic acid treatment for schizophrenia associated with folate receptor autoantibodies. *Mol. Genet. Metab.* **2014**, *113*, 307–314. [[CrossRef](#)]
67. Mercimek-Mahmutoglu, S.; Stockler-Ipsiroglu, S. Cerebral Folate Deficiency and Folinic Acid Treatment in Hypomyelination with Atrophy of the Basal Ganglia and Cerebellum (H-ABC) Syndrome. *Tohoku J. Exp. Med.* **2007**, *211*, 95–96. [[CrossRef](#)]
68. Karin, I.; Borggraefe, I.; Catarino, C.B.; Kuhm, C.; Hoertnagel, K.; Biskup, S.; Opladen, T.; Blau, N.; Heinen, F.; Klopstock, T. Folinic acid therapy in cerebral folate deficiency: Marked improvement in an adult patient. *J. Neurol.* **2017**, *264*, 578–582. [[CrossRef](#)]
69. Al-Baradie, R.S.; Chaudhary, M.W. Diagnosis and management of cerebral folate deficiency. A form of folinic acid-responsive seizures. *Neurosciences* **2014**, *19*, 312–316.
70. Moretti, P.; Sahoo, T.; Hyland, K.; Bottiglieri, T.; Peters, S.; Del Gaudio, D.; Roa, B.; Curry, S.; Zhu, H.; Finnell, R.; et al. Cerebral folate deficiency with developmental delay, autism, and response to folinic acid. *Neurology* **2005**, *64*, 1088–1090. [[CrossRef](#)]
71. Hansen, F.J.; Blau, N. Cerebral folate deficiency: Life-changing supplementation with folinic acid. *Mol. Genet. Metab.* **2005**, *84*, 371–373. [[CrossRef](#)]
72. Frye, R.E.; Donner, E.; Golja, A.; Rooney, C.M. Folinic acid-responsive seizures presenting as breakthrough seizures in a 3-month-old boy. *J. Child Neurol.* **2003**, *18*, 562–569. [[CrossRef](#)]
73. Robinson, A.C.; Palmer, L.; Love, S.; Hamard, M.; Esiri, M.; Ansorge, O.; Lett, D.; Attems, J.; Morris, C.; Troakes, C.; et al. Extended post-mortem delay times should not be viewed as a deterrent to the scientific investigation of human brain tissue: A study from the Brains for Dementia Research Network Neuropathology Study Group, UK. *Acta Neuropathol.* **2016**, *132*, 753–755. [[CrossRef](#)]
74. Chance, S.A.; Esiri, M.M.; Crow, T.J. Ventricular enlargement in schizophrenia: A primary change in the temporal lobe? *Schizophr. Res.* **2002**, *62*, 123–131. [[CrossRef](#)]
75. Horga, G.; Bernacer, J.; Dusi, N.; Entis, J.; Chu, K.; Hazlett, E.A.; Haznedar, M.M.; Kemether, E.; Byne, W.; Buchsbaum, M.S. Correlations between ventricular enlargement and gray and white matter volumes of cortex, thalamus, striatum, and internal capsule in schizophrenia. *Eur. Arch. Psychiatry Clin. Neurosci.* **2011**, *261*, 467–476. [[CrossRef](#)]
76. Melzer, L.; Freiman, T.; Derouiche, A. Rab6A as a Pan-Astrocytic Marker in Mouse and Human Brain, and Comparison with Other Glial Markers (GFAP, GS, Aldh1L1, SOX9). *Cells* **2021**, *10*, 72. [[CrossRef](#)]
77. Miyayama, J.; Cains, S.; Larcombe, S.; Naz, N.; Jimenez, A.R.; Bueno, D.; Gato, A. Subarachnoid cerebrospinal fluid is essential for normal development of the cerebral cortex. *Semin. Cell Dev. Biol.* **2020**, *102*, 28–39. [[CrossRef](#)]
78. Reddy, O.C.; Van Der Werf, Y.D. The Sleeping Brain: Harnessing the Power of the Glymphatic System through Lifestyle Choices. *Brain Sci.* **2020**, *10*, 868. [[CrossRef](#)]
79. Naganawa, S.; Taoka, T. The Glymphatic System: A Review of the Challenges in Visualizing its Structure and Function with MR Imaging. *Magn. Reson. Med Sci.* **2022**, *21*, 182–194. [[CrossRef](#)]
80. Rasmussen, M.K.; Mestre, H.; Nedergaard, M. The glymphatic pathway in neurological disorders. *Lancet Neurol.* **2018**, *17*, 1016–1024. [[CrossRef](#)]

81. Alam, C.; Aufreiter, S.; Georgiou, C.J.; Hoque, T.; Finnell, R.H.; O'Connor, D.L.; Goldman, I.D.; Bendayan, R. Upregulation of reduced folate carrier by vitamin D enhances brain folate uptake in mice lacking folate receptor alpha. *Proc. Natl. Acad. Sci. USA* **2019**, *116*, 17531–17540. [[CrossRef](#)] [[PubMed](#)]
82. Ramaekers, V.T.; Blau, N. Cerebral folate deficiency. *Dev. Med. Child Neurol.* **2007**, *46*, 843–851. [[CrossRef](#)]
83. Ramaekers, V.; Sequeira, J.M.; Quadros, E.V. Clinical recognition and aspects of the cerebral folate deficiency syndromes. *Clin. Chem. Lab. Med. (CCLM)* **2013**, *51*, 497–511. [[CrossRef](#)] [[PubMed](#)]
84. Sadighi, Z.; Butler, I.J.; Koenig, M.K. Adult-Onset Cerebral Folate Deficiency. *Arch. Neurol.* **2012**, *69*, 778–779. [[CrossRef](#)] [[PubMed](#)]
85. Garcia-Cazorla, A.; Quadros, E.V.; Nascimento, A.; Garcia-Silva, M.T.; Briones, P.; Montoya, J.; Ormazabal, A.; Artuch, R.; Sequeira, J.M.; Blau, N.; et al. Mitochondrial diseases associated with cerebral folate deficiency. *Neurology* **2008**, *70*, 1360–1362. [[CrossRef](#)]
86. Serrano, M.; García-Silva, M.T.; Martin-Hernandez, E.; O'Callaghan, M.D.M.; Quijada, P.; Martinez-Aragón, A.; Ormazábal, A.; Blázquez, A.; Martín, M.A.; Briones, P.; et al. Kearns-Sayre syndrome: Cerebral folate deficiency, MRI findings and new cerebrospinal fluid biochemical features. *Mitochondrion* **2010**, *10*, 429–432. [[CrossRef](#)]
87. Willemsen, M.A.A.P.; Wevers, R.; Verbeek, M.M.; Vebeek, M.M. Cerebral Folate Deficiency Syndrome. *N. Engl. J. Med.* **2005**, *353*, 740. [[CrossRef](#)]
88. Iliif, J.J.; Chen, M.J.; Plog, B.A.; Zeppenfeld, D.M.; Soltero, M.; Yang, L.; Singh, I.; Deane, R.; Nedergaard, M. Impairment of Glymphatic Pathway Function Promotes Tau Pathology after Traumatic Brain Injury. *J. Neurosci.* **2014**, *34*, 16180–16193. [[CrossRef](#)]
89. Peng, W.; Achariyar, T.M.; Li, B.; Liao, Y.; Mestre, H.; Hitomi, E.; Regan, S.; Kasper, T.; Peng, S.; Ding, F.; et al. Suppression of glymphatic fluid transport in a mouse model of Alzheimer's disease. *Neurobiol. Dis.* **2016**, *93*, 215–225. [[CrossRef](#)]
90. Lou, Y.; Carlock, C.; Wu, J. Glymphatic Efficiency is a Critical Factor for Using Abnormal Tau in Peripheral Tissues as Biomarker for Alzheimer's Disease. *Biomark. Appl.* **2018**, *2*. [[CrossRef](#)]
91. Harrison, I.F.; Ismail, O.; Machhada, A.; Colgan, N.; Ohene, Y.; Nahavandi, P.; Ahmed, Z.; Fisher, A.; Meftah, S.; Murray, T.K.; et al. Impaired glymphatic function and clearance of tau in an Alzheimer's disease model. *Brain* **2020**, *143*, 2576–2593. [[CrossRef](#)]
92. Lee, Y.; Choi, Y.; Park, E.-J.; Kwon, S.; Kim, H.; Lee, J.Y.; Lee, D.S. Improvement of glymphatic-lymphatic drainage of beta-amyloid by focused ultrasound in Alzheimer's disease model. *Sci. Rep.* **2020**, *10*, 1–14. [[CrossRef](#)]
93. Reeves, B.C.; Karimy, J.K.; Kundishora, A.J.; Mestre, H.; Cerci, H.M.; Matouk, C.; Alper, S.L.; Lundgaard, I.; Nedergaard, M.; Kahle, K.T. Glymphatic System Impairment in Alzheimer's Disease and Idiopathic Normal Pressure Hydrocephalus. *Trends Mol. Med.* **2020**, *26*, 285–295. [[CrossRef](#)]
94. Tice, C.; McDevitt, J.; Langford, D. Astrocytes, HIV and the Glymphatic System: A Disease of Disrupted Waste Management? *Front. Cell. Infect. Microbiol.* **2020**, *10*, 523379. [[CrossRef](#)]

Disclaimer/Publisher's Note: The statements, opinions and data contained in all publications are solely those of the individual author(s) and contributor(s) and not of MDPI and/or the editor(s). MDPI and/or the editor(s) disclaim responsibility for any injury to people or property resulting from any ideas, methods, instructions or products referred to in the content.